JOURNAL OF Applied Polymer SCIENCE

Micro-contact reconstruction of adjacent carbon nanotubes in polymer matrix through annealing-induced relaxation of interfacial residual stress and strain

Dongxu Li,[1,2] Guoxia Fei,[1] Hesheng Xia,[1] Paul E. Spencer,[1] Philip D. Coates[2]

[1]State Key Laboratory of Polymer Materials Engineering, Polymer Research Institute, Sichuan University, Chengdu 610065, China
[2]Polymer IRC, Faculty of Engineering and Informatics, University of Bradford, Bradford BD71DP, United Kingdom
Correspondence to: H. Xia (E-mail: xiahs@scu.edu.cn) and Dr. P. E. Spencer (E-mail: p.e.spencer@bradford.ac.uk)

ABSTRACT: Thermoplastic polyurethane (TPU)/multi-walled carbon nanotubes (CNT) nanocomposites were prepared by twin-screw extrusion and micro injection molding. The electrical conductivity of micro injection molded polymer nanocomposites exhibits a low value and uneven distribution in the micromolded samples. Real-time tracing of electrical conductivity was conducted to investigate the post thermal treatment on the electrical conductivity of microinjection molded composites. The results show that postmolding thermal treatment leads to a significant increase in the electrical conductivity by over three orders of magnitude for 5 wt % CNT-filled TPU composites. *In-situ* Transmission electron microscopy confirms the conductive CNT network does not change at the micron/sub-micron scale during thermal treatment. TEM image analysis by a statistical method was used to determine the spatial distribution of CNT in the sample and showed that the average distance between adjacent CNT reduced slightly at the nanometer scale after postmolding thermal treatment. A new conductive mechanism is proposed to explain the enhancement of electrical conductivity after thermal treatment, i.e. micro-contact reconstruction of adjacent CNT in the polymer matrix through annealing-induced relaxation of interfacial residual stress and strain. Raman spectra and small angle X-ray scattering curve of annealed samples provide supporting evidence for the proposed new conductive mechanism. The electron tunneling model was used to understand the effect of inter-particle distance on the conductivity of polymer composites. © 2015 Wiley Periodicals, Inc. J. Appl. Polym. Sci. **2015**, *132*, 42416.

KEYWORDS: graphene and fullerenes; morphology; nanotubes; properties and characterization; structure–property relations; theory and modeling

Received 9 January 2015; accepted 26 April 2015
DOI: 10.1002/app.42416

INTRODUCTION

Carbon nanotubes (CNT) have drawn much attention as potential nanofillers for polymers due to their mextraordinary mechanical, electrical, and thermal properties.[1–3] Due to their high aspect ratio, low density, and large specific area,[4,5] CNT are regarded as one of ideal candidates for the production of high performance polymer composites. The combination of versatile physical properties from CNT with the flexible processability of polymer stimulated the applications for polymer composites in commercial products, especially for electrically conductive composite materials, including flexible sensors,[6] electrodes,[7] electromagnetic interference (EMI) shielding materials,[8] antistatic materials,[9] and multifunctional shape memory composites.[10]

Electrical properties in polymer composites are often explained by the formation of an interconnected filler network, which transfers the electrical current.[11] With increasing the filler content in a polymer composite, the electrical conductivity of the composite exhibits a sudden increase from insulate to conductive state, at a critical loading of conductive filler is defined as the percolation threshold.[12,13] The formation of conductive pathways in the filler network dominates the electrically conductive behavior of polymer composites above the percolation concentration of conductive filler. For the CNT-filled polymer composites, the percolation behavior strongly depends on the nanotube diameter, length, degree of purification, dispersion state of CNT, and type of matrix polymer.[12,14,15] Meanwhile, as the CNT dispersed in the polymer matrix are usually not directly connected with each other, CNT-polymer-CNT interactions[16] and the insulating region formed by the polymer matrix between CNT[17] play an important role for the transportation of electrons in the conductive network of CNT in CNT/polymer composites.

Additional Supporting Information may be found in the online version of this article.

Apart from the intrinsic properties of CNT and polymer matrix, the blending conditions and processing methods of CNT/polymer composites affect the network formation of CNT in the matrix. In-situ polymerization,[10,18] solution processing,[19] polymer grafting,[20] latex approach,[21] and melt mixing[16,22] were commonly employed for the preparation of CNT/polymer composites. Melt mixing is the most convenient method for the large-scale industrial production. However, the resultant electrical conductivity varies with different processing parameters due to the variations in the dispersion, distribution and orientation of CNT.[23,24] The strong shear stress during melt blending can disperse individual CNT into the matrix, but rupture the agglomerates of CNT, and thus influence the morphology of conductive pathways in the CNT network.

Postmolding thermal treatment has been shown to be an effective method to enhance the electrical conductivity of polymer/conductive filler composites.[24–28] The reaggregation of conductive fillers under high temperature was widely assumed to be responsible for this phenomenon. For example, Alig *et al.*[24,26,27] investigated the recovery of conductivity after annealing for melt processed polypropylene and polycarbonate containing CNT. It is found that for 2 wt % MWNT/PP composites, the conductivity increased from 10^{-7} to 10^{-3} S/m under 220°C for 20 min, and for 0.875 wt % MWNT/PC composites, the conductivity increased from 10^{-10} to 10^{-3} S/m under 260°C for 20 min. The internal network formation after annealing was speculated and several models were established to explain the enhanced conductivity enhancement. Zhang *et al.*[25] found that thermal annealing under high temperatures can reform or reconstruct the conducting networks of CNT in a polyurethane matrix. Secondary agglomeration[11] which is derived from thermodynamic driving forces (e.g., heating induced forces) or external forces (e.g., shear deformation) can lead to inhomogeneous CNT distribution with CNT aggregation, and thus the electrical conductivity improves for CNT/polymer composites. Pan *et al.*[29] found that for microinjection molded 5 wt % MWCNT/PP composites, the electrical conductivity was increased from 10^{-9} to 10^{-3} S/cm under 230°C for 30 min, they observed the morphology evolution of annealed samples and confirmed that reaggregation of MWCNT (transition from individual CNT to loosely packed agglomerate) induced the jump of electrical conductivity. Meanwhile, the disorientation of carbon nanofillers upon annealing and dynamic percolation in highly oriented conductive networks was proposed by Zhang *et al.* to explain annealing induced increased conductivity.[30] Cipriano *et al.*[31] found that for compression molded 4 wt % MWCNT/PS composites, the electrical conductivity was increased from 10^{-8} to 10^{-2} S/m under 170°C for 30 min, and they revealed the transition of conductive network from aligned, unconnected particles to an interconnected network before and after annealing. The reaggregation of CNT under annealing at a temperature above the melting point which leads to CNT network reconstruction is possible, however, up to now, no direct evidence for the reconstruction of conductive network change after annealing, e.g., *in situ* observation results, has been reported. TEM images showing the re-aggregation of CNT after annealing at a higher temperature are usually taken from two different positions of the samples.

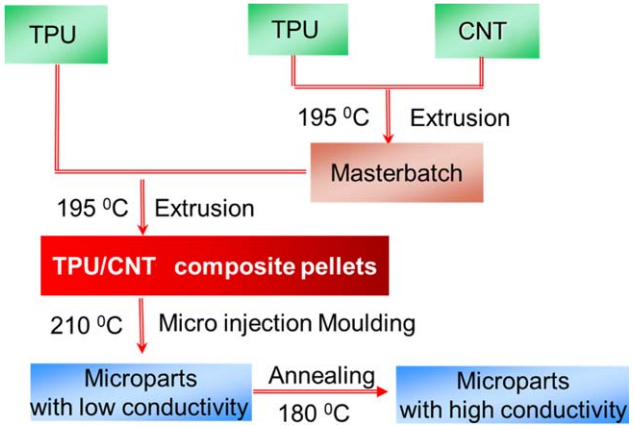

Scheme 1. Preparation and processing of polyurethane/CNT nanocomposite. [Color figure can be viewed in the online issue, which is available at wileyonlinelibrary.com.]

In this study, we report that thermal treatment can improve the electrical conductivity of CNT filled TPU composite samples obtained by microinjection molding. *In situ* TEM was used to observe the internal CNT conductive network change in the polymer matrix during thermal treatment from room temperature to melting temperature. The conductive CNT network does not change in the micron/sub-micron scale, and further quantitative analysis showed that the average distance between adjacent CNT reduced slightly at a size scale of several nanometers after postmolding thermal treatment. Based on our experimental observations, a new conductive mechanism is proposed to explain the enhancement of electrical conductivity, i.e., reconstruction of conductive pathways in the CNT network in polymer through annealing-induced removal of interfacial residual stress and strain. To the best of our knowledge, the mechanism related to the interfacial residual stress and strain on the post thermal treatment induced enhancement on the electrical conductivity of polymer composites has never been reported. The microinjection-molded polymer/CNT nanocomposites were used for the investigation as these samples have large residual stresses and strains due to the high temperature gradient and high shear rate gradient imposed in microinjection molding processing.

EXPERIMENTAL

Materials

The thermoplastic polyurethane elastomer (ESA-480) with a shore hardness of 80A is a commercial grade purchased from Shenzhen Pepson Company, China. The pristine multi-walled carbon nanotubes (C7000) supplied by Nanocyl SA (Belgium) had an average diameter of ~9.5 nm, length of ~1.5 μm, and Carbon Purity of ~90%. The carbon nanotubes were directly used without any pretreatment.

Preparation of Polyurethane/CNT Nanocomposite by Melt Mixing

The polyurethane/CNT nanocomposite pellets for microinjection molding were prepared through a masterbatch and dilution approach. The preparation process is illustrated in Scheme 1. First, the masterbatch with a higher weight

concentration of 12% CNT were produced by melt extrusion. The experiments were conducted by using a SHJ-25 extruder with twin co-rotating screws (CM Plastics Machinery Industry, China) at a barrel temperature of 195°C and a screw speed of 120 rpm. The extruded material was cooled down to room temperature in a water bath and granulated afterwards. All the materials used were dried in a vacuum oven at 100°C for at least 2 h before each processing step. Then the polyurethane/CNT nanocomposite with different weight concentrations, 1, 3, 5% was extruded, cooled, and granulated under the same processing conditions by using the masterbatch pellets.

Micro Injection Molding of TPU/CNT Nanocomposites Pellets

The obtained TPU/CNT nanocomposites pellets were micromolded into dumbbell-shaped microparts (tensile bar) by a Haake Mini-jet machine (Thermo Electron Corporation, Germany). The experimental parameters for the micro-injection molding process are as follows: melting temperature ~210°C, mold temperature ~25°C, injection pressure ~77 MPa, holding pressure ~20 MPa and holding time ~10 s. Compression molding and conventional injection molding were also conducted in order to investigate the effect of different processing methods on the electrical conductivity of the materials.

To improve the electrical conductivity of microinjection molded TPU/CNT nanocomposites, samples were thermal treated at a constant temperature (45, 70, 100, 130, 150, 180, and 205°C) for a certain time and then cooled down to room temperature.

Compression Molding

The mixed TPU/CNT nanocomposites pellets were put into a mold with a 2 mm deep cavity and kept at 210°C for 5 min under a pressure of 10 MPa. The force was released to zero twice in order to remove the gas in the sample. Finally the pressed samples were cooled and kept at 25°C for 5 min under a pressure of 10 MPa.

Conventional Injection Molding

Standard tensile bars were obtained by conventional injection molding with a PS40E5ASE precise injection-molding machine (Nissei, Japan). The experimental parameters for the injection molding process were as follows: melting temperature ~210°C, mold temperature ~25°C, injection pressure ~35 MPa, holding pressure 20 MPa and holding time ~10 s.

Characterization

The electrical conductivity of all samples was measured by a simple two-point measurement with a picoameter (Keithley 2400). Electrodes were painted onto the rectangle sample strip using silver epoxy paste. The measured volume resistance (R_v) was converted to volume electrical conductivity (σ_v) according to the standard (ASTM D4496 and D257) using the formula:

$$\sigma_v = \frac{t}{A * R_v} \quad (1)$$

where R_v is the measured resistance (Ω), A is the effective area of the measuring electrode (m^2), and t is specimen thickness (m).

TEM was performed using a FEI Tecnai G^2 F20 S-TWIN transmission electron microscope, operating at an accelerating voltage of 200 kV. The CNT/TPU composites were cryo-microtomed using a Leica EM UC6 equipment to get the ultra-thin cryo-sections of 70−80 nm thickness, which were collected and directly supported on a copper grid for observation.

Raman imaging was performed on a Jobin–Yvon Horiba Labram HR spectrometer using a 633 nm excitation wavelength (HeNe laser). A long-working distance objective with magnification 50× was used both to collect the scattered light and to focus the light beam of laser operating at 633 nm to a spot with appropriate diameter of 2 μm on the sample surface.

Small angle X-ray scattering investigation was carried out at BL16B1 beam-line at Shanghai Synchrotron Radiation Facility (SSRF), China. Briefly, the sample to detector distance was 2030 mm, the wavelength of the beamline was 0.124 nm, the exposure time for each image was 20 s, and the scattering vector q was in the range of 0.15−2.9 nm^{-1}. The samples were heated and cooled within the SAXS chamber and the heating and cooling rates were fixed at 10°C/min.

RESULTS AND DISCUSSION

Effect of Post Treatment on the Electrical Conductivity of the Composite

The big challenge in preparing electrical conductive TPU/CNT nanocomposite products is the formation of CNT networks with good contact between the adjacent CNT. Polymer sheathing of CNT should be avoided due to it hampering of the CNT contact. The thermal melt processing with shear force has important effects on the formation CNT network and thus the electrical conductivity of CNT-polymer composite.

Figure 1(a) shows the effect of different processing methods on the electrical conductivity of nanocomposites. Without any thermal treatment, the microinjection molded micropart exhibits much lower electrical conductivity, compared to the samples obtained from conventional injection molding and compression molding. It is recognized that the network formation of CNT in polymer matrix varies with different processing methods.[32] For micromolded microparts made from polymer/CNT nanocomposites, it is difficult to reach a good electrical conductivity. Due to the high shear rate and rapid cooling rate, the micromolding process severely breaks down the conductive network and contact of CNT, despite that this process facilitates the dispersion of CNT in the polymer melt. Consequently, the electrical conductivity of molded parts is much lower than the thermal pressed one or conventional injection-molded one. Also the electrical conductivity at three different sites, position A1, A2, and A3 along the injection direction were compared as shown in Figure 1(a). Position A3 which is far from the injection gate has the highest electrical conductivity as much as 0.0178 S/m among the three positions, while the position A1 close to the injection gate has the lowest conductivity of 0.0031 S/m, lower by around one order of magnitude. This also can be attributed to the different shear effect at different sites in the same sample. Close to the injection gate, the shear effect of the polymer/CNT nanocomposite melt is more severe compared to other two sites, and therefore an intact CNT network is more difficult to form or retain. Also, for position A3, longer

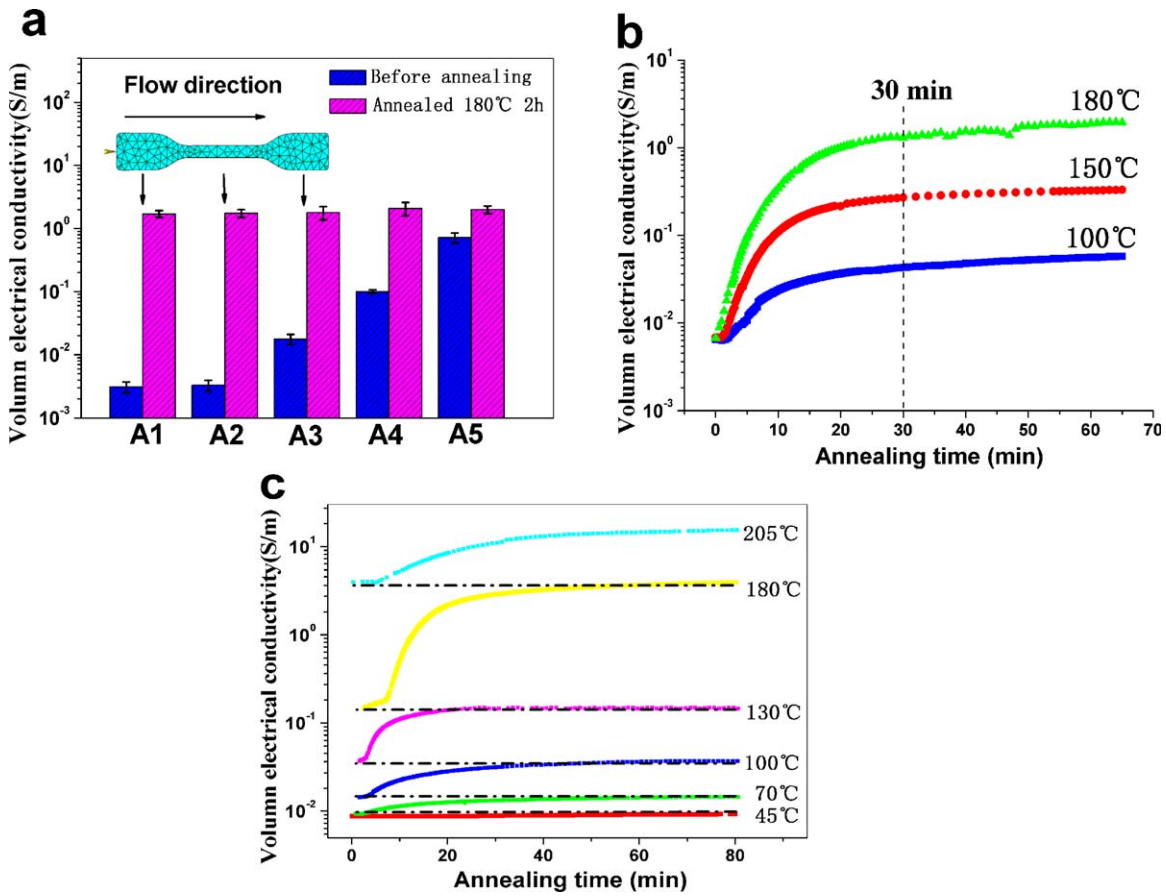

Figure 1. (a) The electrical conductivity for 5 wt % CNT/TPU composites: A1-A3 represent three different positions along the flow direction of micro injection-molded sample, A4 represents the sample processed by conventional injection molding, A5 represents the sample processed by compression molding. (b) The increase in the conductivity for A2 with the time after thermal treatment at a constant temperature 100, 150, and 180°C. (c) The increase in the conductivity for A2 with the time after thermal treatment at a constant temperature 45, 70, 100, 130, 180, 205°C. [Color figure can be viewed in the online issue, which is available at wileyonlinelibrary.com.]

retention of polymer melt creates more time for the polymer chains to equilibrate and causes the highest electrical conductivity. Fortunately, we found that the issues about low electrical conductivity for microinjection molded parts and the nonuniform conductivity distribution can be solved through a post-molding thermal treatment process. As shown in Figure 1(a) the electrical conductivity of the nanocomposites exhibits an extraordinary transition after post-molding thermal treatment, i.e., annealing at 180°C for 2 h. After thermal treatment, the values of electrical conductivity for all samples obtained by different approaches and at different sites improve to the similar values, over 1 S/m.

Figure 1(b) shows the volume electrical conductivity for 5 wt % CNT/TPU composites versus time under isothermal treatment at a constant temperature of 100, 150, and 180°C, respectively. Clearly, the conductivity for all three samples increases with time and reaches a thermal equilibrium value during the isothermal annealing process. For example, after annealing at 180°C for 30 min, the electrical conductivity increases significantly from $\sim 7 \times 10^{-3}$ to 1.3 S/m by approximately three orders of magnitude. Also we found that with increasing annealing temperature, the composites show a more rapid increase in the conductivity and a higher equilibrium conductivity value.

The increase in the volume electrical conductivity with the time for annealing temperatures in the range 45−205°C was further measured and the data are shown in Figure 1(c). The sample was firstly thermal treated under 45°C for 80 min and cooled down to room temperature. Then the sample was thermal treated again under 70°C for another 80 min and also cooled down to room temperature. The same procedure was further performed at 100, 130, 180, and 205°C. All the electrical conductivity values were determined for each temperature as shown in Figure 1(c). The results show that the final conductivity of the nanocomposites is dependent on the thermal treatment temperature, and also indicate that the conductivity can be controlled by adjusting the thermal treatment temperature.

The Electrical Conduction Mechanism for Annealing-induced Enhancement in the Electrical Conductivity

Reagglomeration of CNT and reconstruction of the conductive network in the melt during thermal treatment were proposed and several models were used to explain this phenomenon.[24–28] In order to elucidate the conduction mechanism for TPU/CNT

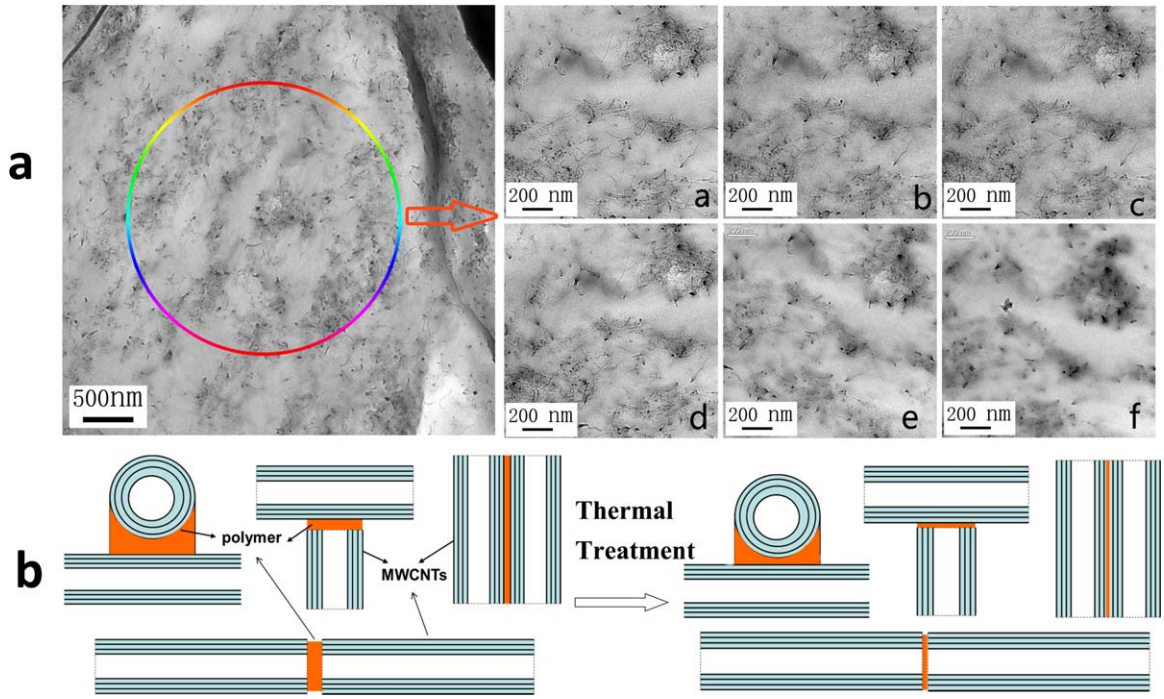

Figure 2. (a) TEM images of 5 wt % CNT/TPU composites under different temperatures during *in-situ* thermal treatment process (a: 22, b: 54, c: 78, d: 95, e: 180, f: 205°C). (b) Schematic illustration for annealing induced interfacial change in the adjacent CNT. [Color figure can be viewed in the online issue, which is available at wileyonlinelibrary.com.]

composites after thermal treatment, we employed an *in-situ* TEM technique to characterize the internal CNT structure change, from low to high annealing temperature. The experiment was performed using a TEM machine equipped with a temperature control unit. During the observation, the sample was heated from 22 to 205°C at a rate of 5°C/min and held for 2 h.

The TEM images shown in Figure 2(a) were taken at different temperatures: 22, 54, 78, 95, 180, 205°C. From Figure 2(a), it seems that the CNT network at the micron- or submicron-scale level remains stable and no CNT movement from random dispersion to agglomerates was found during the thermal treatment process, even at 180 and 205°C for 2 h. This result is different from the case by Alig *et al.*[28] which showed that after annealing treatment for 0.6 vol % (below percolation threshold) MWCNT/PC nancomposites at 300°C, the MWCNT will reagglomerate to form the submicron aggregates and lead to a CNT network reconstruction and thus enhance the conductivity from $\sim 10^{-10}$ to $\sim 10^{-3}$ S/cm. In our study, the significant conductivity enhancement during thermal treatment could not be attributed to the CNT network reformation as the CNT network does not change at a micron/submicron scale.

Normally, there are two main mechanisms to account for the electrical conduction of polymer/CNT nanocomposites: (1) percolation mechanism; and (2) electron tunneling mechanism. Percolation is the formation of long-range connectivity of conductivity fillers in random systems. Above the percolation threshold, there exists a large scale connected component of the order of the system size. In this case, the conductivity of the composites transforms from insulating to conducting. The electrical conductivity can be fitted by a scaling law:

$$\sigma = \sigma_0 \cdot (\varphi - \varphi_c)^{t'} \quad (2)$$

where φ_c is the percolation threshold concentration of fillers, and t' is system dimensionality. Electron tunneling is very important for the electron transfer. Electrons in a polymer cannot normally transfer from one electrode to another through an insulator due to an energy barrier. The electronic current can flow only if: (a) the electrons have enough energy to surmount the potential barrier; (b) the barrier is thin enough to permit its penetration by the electric tunnel effect. For CNT/polymer composites, the thickness of interfacial polymer between adjacent conductive CNT is an important factor for electron tunneling. In order to better understand the annealing-induced enhancement in the conductivity, based on our experimental observations, we proposed the following two hypotheses:

Hypothesis I. When the CNTs/polymer composites were subjected to the shearing processing such as extrusion, injection molding, there will be significant increase in the interfaces between CNTs and polymer during the intense mixing, and the CNTs contact will be broken to some degree. Once the shearing processing is stopped and the sample is cooled, residual stresses and strains will exist in the polymer matrix and also in the interfacial polymer between CNT, as a result of cooling shrinkage mismatch of CNT and polymer. Actually the extruded or injection-molded plastic parts are in a nonequilibrium state due to the existence of residual stress. The presence of interfacial polymer hampers the formation of electrical conductivity

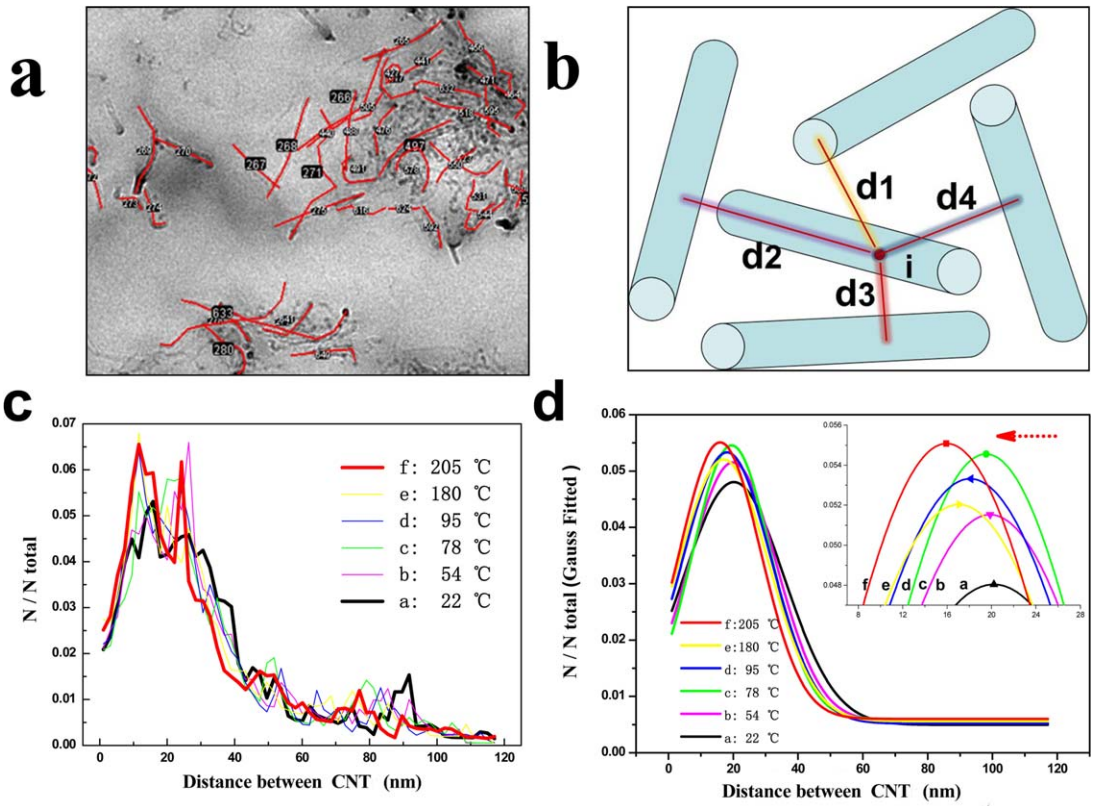

Figure 3. (a) Example of CNT identification from a TEM image of 5 wt % CNT/TPU composite. (b) Schematic drawing of nearest neighbor particle distance for CNT/TPU composite. (c) The normalized histogram data of nearest neighbor particle distance distribution for 5 wt % CNT/TPU composites treated under different temperatures. (d) The fitted curves with Gaussian function for N/N_{total} as a function of the distance. [Color figure can be viewed in the online issue, which is available at wileyonlinelibrary.com.]

pathways, it is reasonable that some CNT in the polymer matrix are sheathed or encapsulated by polymer chains which prevent the electrons from "jumping" between CNT. Fewer conductive pathways lead to decreased electrical conductivity.

Hypothesis II. During the post thermal treatment, when the temperature rises above T_g, the polymer chain is relatively free to move. The interfacial elastic polymer with a residual strain at the surface of CNT may contract back to the matrix and the shrinkage of the polymer layer will decrease the distance between two CNT, which promotes the tunneling conduction and enhances the electrical conductivity significantly, as shown in Figure 2(b). We deduced the CNT separation distance changes in the nano-scale and will not affect the micron-level CNT network structure.

We found some evidences as follows to support the hypothesis of interfacial polymer layer structure change.

Inter-Particle Distances Analysis. TEM image analysis by a statistical method was used to determine the spatial distribution of CNT in the sample during post thermal treatment. TEM is the most effective method to look into the nanolevel structure and dispersion of fillers in polymer matrix. Few quantitative statistical methodologies of filler dispersion based on TEM images were reported. Vermogen *et al.*[33] proposed a statistical analysis methodology to describe the clay dispersion in polypropylene based on the definition of different tactoid classes, the average lengths, thicknesses and extent of agglomeration were obtained. Luo *et al.*[34] presented a methodology, which gives a "free-path distance" to quantify the layer dispersion degrees from TEM images. Basu *et al.*[35] and Xie *et al.*[36] developed a quantitative TEM characterization method using stereology to evaluate the mean inter-particle distance (the average distance between every possible combination of particles) for clay/polymer composites.

The Monte Carlo method was used in our analysis to obtain relevant distances from TEM images and determine the spatial distribution of CNT in annealed CNT/TPU composites. The *in-situ* TEM images for the sample obtained at different annealing temperatures: 22, 54, 78, 95, 180, and 205°C were chosen for analysis. The analytical process is illustrated in Scheme S1. First, we identified individual CNT and traced segmented-lines along the "backbone" of each particle visible in the images as is shown in Figure 3(a) and Supporting Information Figure S1. Second, the coordinate information for the exact same CNT in 6 TEM images was obtained. Third, the coordinate data are imported into a self-developed programme compiled in python language. A spatial-distribution function based on distances between pairs of points as a function of scale was developed to characterize the particle clustering and dispersion. More details for quantitative inter-particle analysis based on TEM images can be found in the supporting information.

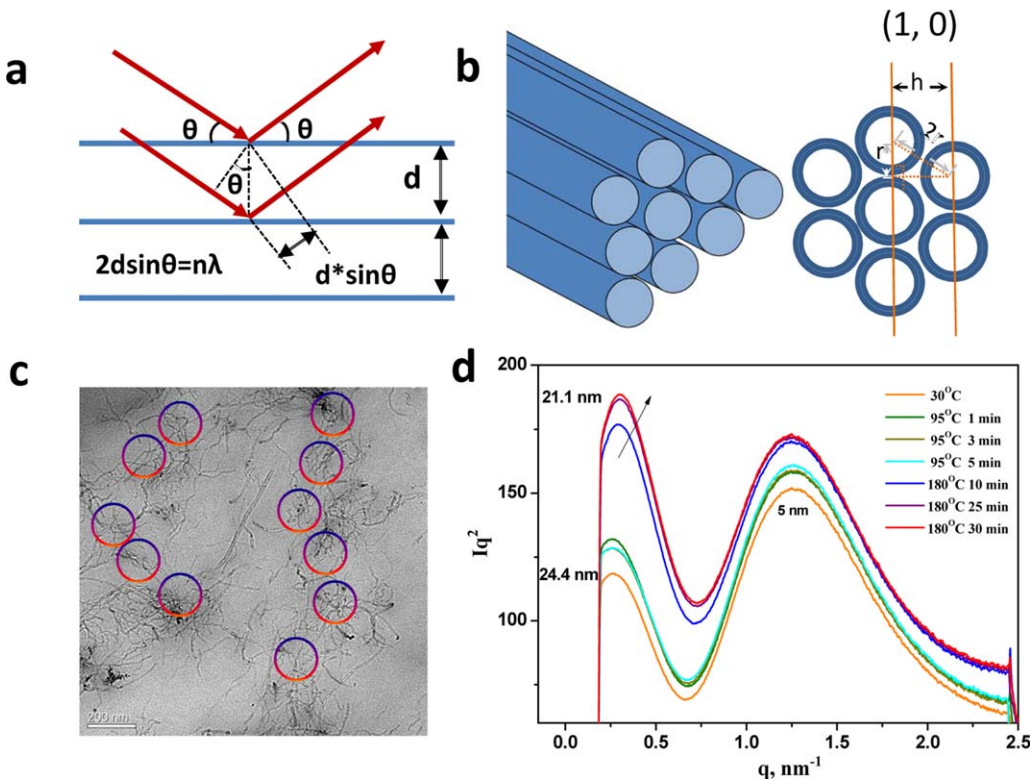

Figure 4. (a) Schematic illustration for the Bragg law, X-rays (arrows) are reflected by crystallographic planes separated by a distance d, λ is the wavelength of the X-rays, 2θ is the scattering angle, n is an integral number. (b) Scheme for hexagonal crystal lattice characteristic of CNT bundle, the diameter of each CNT is 2r. "h" is the d-spacing of (1, 0) planes. (c) TEM images of 5 wt % CNT/TPU composites showing the existence of CNT bundles. (d) The evolution of Lorentz-corrected SAXS pattern of 5 wt % CNT/TPU composite during annealing. Iq^2 versus q, where I is the diffraction intensity and q is the scattering vector. The sample was heated under 90°C for 1, 3, and 5 min, and then further heated under 180°C for 10, 25, and 30 min. [Color figure can be viewed in the online issue, which is available at wileyonlinelibrary.com.]

Two independent parameters, nearest-neighbor particle distance and nearest-neighbor distribution were developed. Nearest-neighbor particle distance (d_N) as illustrated in Figure 3(b) is defined as the distance from an arbitrary point along the backbone of an arbitrary particle to its nearest neighbor particle. The nearest-neighbor distribution characterizes the probability of finding a nearest neighbor particle at a given distance from an arbitrary particle.

Figure 3(c) illustrates the probability of finding a nearest neighbor particle at a given distance from an arbitrary particle (N/N_{total}) as a function of distance (d_N). In order to measure the position and distribution of the peaks presented in Figure 3(c), the data for the nearest-neighbor distribution was fitted to the Gauss function over the entire range of d_N as shown in Figure 3(d).

From the results of Figure 3(c), it can be seen that the probability (N/N_{total}) for the small distances ranging from 0 to 20 nm, exhibited an increasing tendency with increasing temperature. For example, when the sample is under 22°C, N/N_{total} is 4.09% for 11.6 nm, after thermal treatment under 95°C and 180°C, the values reach 6.40% and 6.80%, respectively. However, for the distances ranging above 30 nm, the probability data exhibits a reverse trend.

The fitted data in Figure 3(d) can better reflect the change before and after thermal treatment. The N/N_{total} value increases with temperature at the region with a distance below 22 nm, positions of the peak from the curve-fits were 20.2, 19.9, 19.5, 18.1, 17.1, and 16.0 nm for 22, 54, 78, 95, 180, and 205°C respectively. The position of peak reduces ~4.2 nm after the post thermal treatment. The corresponding maximum probability also increases from 4.8% (22°C) to 5.5% (205°C), which indicates more CNT having a smaller distance with neighbor CNT. TEM image analysis provides an evidence for hypothesis II, i.e. the interfacial polymer layer between CNT become thinner after post thermal treatment.

CNT Bundle Size Analysis by Small Angle X-ray Scattering. Because of chemical affinity CNT sample often consists of aggregates, frequently referred to as bundles, in which from several to tens of single nanotubes self-assembled in a two-dimensional hexagonal lattice held together by van der Waals interaction.[37] As the graphite sheet can be considered to be the reflection layers for X-rays, according to Bragg's law which is presented in Figure 4(a), small angle X-ray scattering (SAXS) has been widely used to evacuate the nature and aggregation level of CNT at different length scales.[38–42] For example, the hierarchy of structures includes single CNT, bundles of CNT and aggregates of CNT bundles in polymer composites can be characterize by SAXS according to García-Gutiérrez's research.[40] Gabriella *et al.*[41] used the SAXS method to analysis the

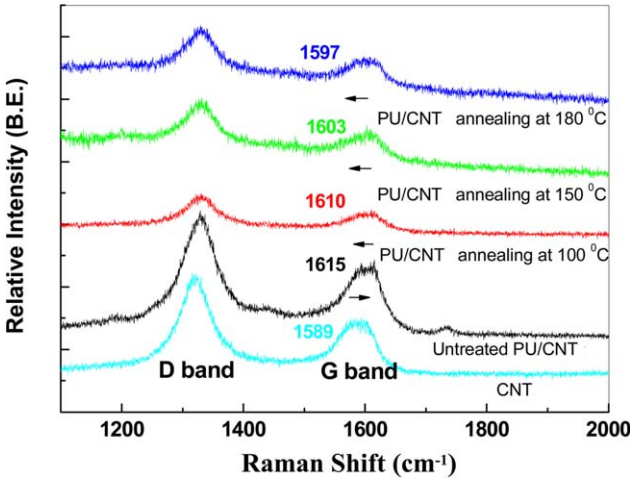

Figure 5. Raman spectra of microinjection molded 5 wt % TPU/CNT composites after annealing at different temperatures. [Color figure can be viewed in the online issue, which is available at wileyonlinelibrary.com.]

different dispersion status of CNT in epoxy composites, i.e. nanotubes in bundles and in micron-sized clusters. SAXS can also be an efficient tool to measure CNT dimensions and orientation, averaged over millions of CNT captured by the beam spot, according to the research of Benjamin *et al.*[42] Martone *et al.*[38] reported that for the CNT with an average diameter of 10 nm, two knee-scattering features corresponding to the size of 6–8 nm and 35 nm assessed as $d = 2\pi/q$ were found, they thought that the dimension of 6−8 nm corresponds to the cross-section of CNT, while the dimension of ∼35 nm can be associated to a bundle consisting of about three nanotubes side-by-side interacting.

Figure 4(b) presents the hexagonal crystal lattice characteristic of CNT bundles, the diameter of each CNT is 2r and "*h*" is the distance of (1, 0) planes.[40] Figure 4(c) is the TEM images of 5 wt % CNT/TPU composites showing the existence of CNT bundles. To speculate the change of CNT bundle morphology and size, SAXS was performed on CNT/TPU composites and the Lorentz corrected SAXS pattern of samples under different temperatures were shown in Figure 4(d). The peak at q_{max}∼1.256 corresponds to the characteristic (1, 0) reflection of a closely packed two-dimensional hexagonal lattice and $q_{max} \sim 0.255$ corresponds to the size of CNT bundle. No shift of peak positions was found for $q_{max} \sim 1.256$ during thermal treatment. However, peak positions for $q_{max} \sim 0.255$ shifts to 0.298 after thermal treatment under 180°C for 30 min.

The corresponding distance of (1, 0) planes and size of CNT bundle can be calculated by Bragg's law $d = 2\pi/q$. Result shows that after thermal treatment under 90°C for 1, 3, and 5 min, the size of CNT bundle remains nearly constant at ∼24.4 nm, however, with further treatment under 180°C for 10, 25, and 30 min, the size of CNT bundle reduces to ∼21.8, 21.3, and 21.1 nm, respectively. This change is nearly in consistent with the above TEM image analysis. The reduced bundle size indicates the possibility of more direct contact or lower tunneling barrier between adjacent CNT in the bundles, which derives from the relaxation of interface elastic polymer with a residual strain at the surface of CNT during thermal treatment. This finding also provides important evidences for our Hypothesis II, i.e. the reduction in the distance between adjacent CNT at a nanosize scale after post thermal treatment occurs, which promotes the reconstruction of micro-contact in the conductive pathways of the CNT network.

Residual Stress and Strain Analysis by Raman Spectra. The Raman band frequency, intensity and shape can vary when CNT interact with other species. This can be used to examine the interface structure and obtain information about the force of interaction.[43–46] The most important Raman bands of CNT included the radial breathing mode (RBM), D band, and G-band. The G band of CNT usually ranges from 1520–1590 cm^{-1} and associates with tangential vibrations of carbon atoms. To be more specific, the G band consists of G^+ band (∼1590 cm^{-1}) and G^- band (∼1565 cm^{-1}). The G^+ band is sensitive to strain. It shifts to lower wave numbers when the CNT are in tension and to higher wave numbers in compression.[44,45]

The Raman spectra of CNT/polyurethane composites are shown in Figure 5. After introducing the CNT into PU, the G band frequency of CNT shifts from 1589 cm^{-1} to a higher wavenumber of ∼1615 cm^{-1}. The upward shift by ∼26 nm in the G-band frequency of CNT indicates the presence of compressive strain on the CNT.[44,45] The strain rises from the residual stress during the cooling process of microinjection-molded polymer composites due to the difference in the thermal expansion coefficients of CNT and polymers. However, after thermal treatment, the G band shifts back to the wavenumber of original CNT which indicates the release of residual stress inside the composites. An increase in the annealing temperature will lead to a larger shift in the G-band frequency of CNT. For example, after annealing at 180°C for 2 h, the G band frequency of CNT in TPU shifts back to 1597 cm^{-1}, close to 1589 cm^{-1} of the original raw CNT. The downward shift of G-band frequency to original CNT suggests the interaction between carbon nanotube and polymer becomes weaker during the annealing process due to the reduction of compressive strain on the CNT.

The upshift and downshift of CNT Raman G-band indirectly confirms that residual stresses and strains indeed exist in the interfacial polymer between CNT and can be released by the thermal treatment process. This provides important evidences for our Hypothesis I and II, i.e. interfacial residual stress and strain is existed in the interfacial polymer layer and can be removed after post thermal treatment. The interfacial residual strain relaxation will promote the micro-contact re-construction of CNT, and thus enhances the electrical conductivity of the materials.

Understanding of the Effect in the Tiny Change of CNT Inter-Particle Distance on the Electrical Conductivity of Composites by Electron Tunneling-Percolation Model

The tunneling-percolation model was widely used for explaining the electrical conductivity behavior of the particle or fiber-filled composites.[47] For the CNT filled polyurethane composites, the adjacent CNT are separated by an insulating polymer layer which creates an energy barrier to electron transfer. The electronic current can flow only if the electrons have enough energy

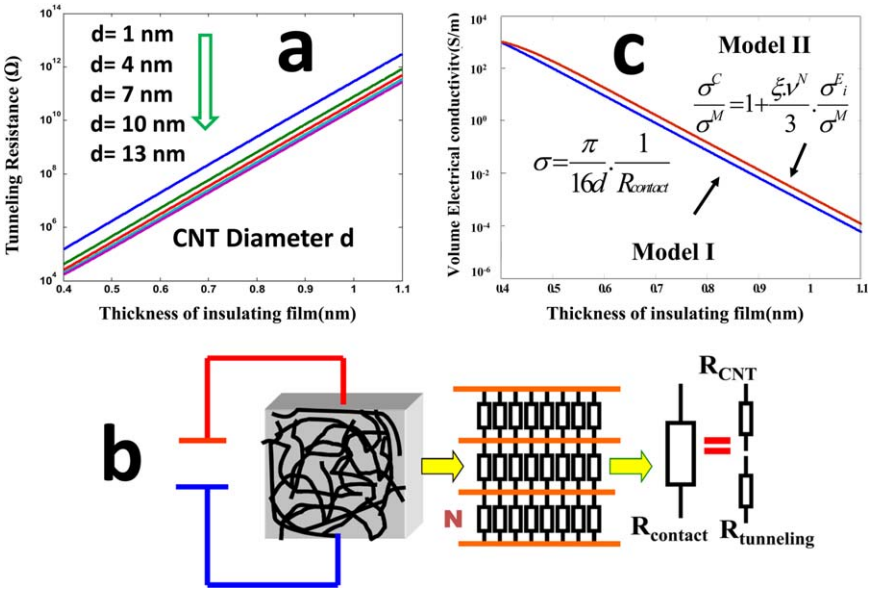

Figure 6. (a) Contact resistance due to electron tunneling as a function of the thickness of polymer layer between adjacent CNT. (b) Schematic illustration for CNT/polymer composites in Model I. (c) Electrical conductivity of CNT/polymer composites as a function of the thickness of polymer film between adjacent CNT. [Color figure can be viewed in the online issue, which is available at wileyonlinelibrary.com.]

to surmount the potential barrier or the barrier is thin enough to permit its penetration by the electric tunnel effect. Simmons's equations[47] predict the electrical tunneling resistance between two planar electrodes separated by a thin insulating layer. In our analysis, the junction is modeled as two planar electrodes separated by a polymer film with effective area of d^2 (d is the diameter of CNT). The resistance of CNT-polymer-CNT junction therefore can be estimated according to the calculating method derived from Yu[48] and Li's work.[17] The tunneling resistance of CNT-polymer-CNT as a function of the thickness of polymer insulating layer and the CNT diameter was predicted as illustrated in Figure 6(a). The results show that the tunneling resistance decreases with increasing CNT diameter, moreover, the thickness of insulating layer plays the most important role in the conductive behavior of composites. It is noted that the tunneling resistance between polymer and CNT increases significantly by several orders of magnitude when polymer layer thickness is increased very slightly.

On the basis of Figure 6(a), the effect of polymer insulating thickness between adjacent CNT on the electrical conductivity of the composites was further speculated using the following two models. Details of the models are as follows:

Model I. The composite assumed as a stacking of layers and the resistance of one layer is that of a network of parallel resistors as shown in Figure 6(b). Each resistor has the same resistance, noted as R_{contact} and represents the contact between the CNT with a polymer film in their vicinity along with the segment of CNT between contacts. The thickness of one layer is assumed to be equal to the distance between contacts, denoted as k. A composite sample of thickness e is a stacking of e/k layers. The electrical resistance is:[49]

$$R=\frac{e}{k}\cdot\frac{R_{contact}}{N} \tag{3}$$

where N denotes the number of contacts (in parallel) in one layer. Considering a composite sample of surface area S, the electrical conductivity is thus obtained:

$$\sigma=\frac{1}{R}\cdot\frac{e}{S}=\frac{k}{e}\cdot\frac{nkS}{R_{contact}}\cdot\frac{e}{S}=\frac{nk^2}{R_{contact}} \tag{4}$$

where n is the number of contacts per unit volume in a three-dimensional random network which is given by:

$$n=\frac{4\varnothing^2}{\pi d^3} \tag{5}$$

where Φ denotes the volume fraction of carbon nanotube and d the diameter of carbon nanotube.

The distance k between contacts in a three-dimensional random CNT network is given by:

$$k=\frac{\pi d}{8\varnothing} \tag{6}$$

Finally, the electrical conductivity of the composite is derived as:

$$\sigma=\frac{\pi}{16d}\cdot\frac{1}{R_{contact}} \tag{7}$$

The resistance of a contact is the sum of R_{CNT} (the resistance of carbon nanotubes) and $R_{\text{tunneling}}$ (the tunneling resistance of CNT-polymer-CNT):

$$R_{contact}=R_{CNTs}+R_{tunneling} \tag{8}$$

Model II. For composites of randomly oriented straight nanotubes, the analytical expression for the electrical conductivity of the composites σ^C with nanotube volume fractions above the percolation threshold is given as:[50,51]

$$\frac{\sigma^c}{\sigma^M}=1+\frac{\delta\nu^N}{3}\cdot\frac{\sigma_i^E}{\sigma^M} \tag{9}$$

where σ^M is the electrical conductivity of the matrix material, ξ is the parameter which is dominated by the percolation threshold and volume content of filler (V^N). $\sigma^E{}_i$ is the longitudinal electrical conductivity of the effective CNT which is given as:

$$\sigma_i^E = \frac{4l_i^E}{\pi(d_i^E)^2 R_i^E} \quad (10)$$

where $l^E{}_i$ is the CNT length and $d^E{}_i$ is the CNT diameter. $R^E{}_i$ is the sum of R_{CNT} (the resistance of carbon nanotubes) and $R_{tunneling}$(the tunneling resistance of CNT-polymer-CNT).

The thickness of insulated polymer between CNT as a function of CNT-based polymer composites described by two models is shown in Figure 6(c). It can be noted that even ~0.1 nm's decrease of polymer thickness between CNT can induce a significant increase in electrical conductivity by ~50%, due to the decrease of tunneling resistance. According to the statistical results of TEM image analysis, more CNT are having smaller distances with neighbor CNT during annealing. For example, with increasing the thermal treatment temperature from 22°C to 180°C, the probability of finding a nearest neighbor CNT increases from 4.1% to 6.8% when the distance is 11.6 nm, while positions of the peaks from the curve-fits decreases from 20.2 to 17.1 nm. Therefore, according to the above electron tunneling-percolation model, it can be understood that those nanoscale movements of adjacent carbon nanotubes during thermal treatment will reduce the tunneling resistance significantly and enhance the electrical conductivity of CNT/polymer composites by several orders of magnitude.

CONCLUSIONS

The electrical conductivity of CNT/TPU composites obtained by micro injection molding was enhanced significantly after thermal treatment. *In-situ* TEM observation confirmed that conductive CNT network under thermal treatment does not change in the micro/sub-micron level. A new conductive mechanism is proposed for the enhancement of electrical conductivity after thermal treatment., i.e. micro-contact re-construction in the conductive pathways of CNT network in the polymer matrix through annealing-induced relaxation of interfacial residual stress and strain, Three findings support our hypothesis: (1) *in-situ* TEM image analysis by a statistical method suggests that the average adjacent CNT distance reduced slightly at a size scale of several nanometers after post thermal treatment; (2) small angle X-ray scattering of annealed sample indicates that the size of CNT bundles decrease with increasing temperature; (3) the shift of the CNT Raman G-band confirms the existence of residual stress and strain in the interfacial polymer between CNT and can be released by thermal treatment. The effects in the tiny change of CNT inter-particle distance on the electrical conductivity of composites are understood by an electron tunneling-percolation model.

ACKNOWLEDGMENTS

H.S. Xia acknowledges financial support from the major project of Chinese Ministry of Education (313036) and National Natural Science Foundation of China (NNSFC, Grant No: 51433006) and the RCUK China-UK Science Bridges Programme. P D Coates and P E Spencer acknowledge support from the RCUK and ESPRC Science Bridges China and Global Engagements Programmes.

REFERENCES

1. Koerner, H.; Price, G.; Pearce, N. A.; Alexander, M.; Vaia, R. A. *Nat. Mater.* **2004**, *3*, 115.
2. Ramasubramaniam, R.; Chen, J.; Liu, H. *Appl. Phys. Lett.* **2003**, *83*, 2928.
3. Kashiwagi, T.; Grulke, E.; Hilding, J.; Groth, K.; Harris, R.; Butler, K.; Shields, J.; Kharchenko, S.; Douglas, J. *Polymer* **2004**, *45*, 4227.
4. Breuer, O.; Sundararaj, U. *Polym. Compos.* **2004**, *25*, 630.
5. Sandler, J. K. W.; Kirk, J. E.; Kinloch, I. A.; Shaffer, M. S. P.; Windle, A. H. *Polymer* **2003**, *44*, 5893.
6. Xia, L.; Wei, Z.; Wan, M. *J. Colloid Interface Sci.* **2010**, *341*, 1.
7. Hou, Y.; Cheng, Y.; Hobson, T.; Liu, J. *Nano Lett.* **2010**, *10*, 2727.
8. Liu, Z.; Bai, G.; Huang, Y.; Ma, Y.; Du, F.; Li, F.; Guo, T.; Chen, Y. *Carbon* **2007**, *45*, 821.
9. Byrne, M. T.; Gun'ko, Y. K. *Adv. Mater.* **2010**, *22*, 1672.
10. Fei, G.; Li, G.; Wu, L.; Xia, H. *Soft Matter* **2012**, *8*, 5123.
11. Alig, I.; Pötschke, P.; Lellinger, D.; Skipa, T.; Pegel, S.; Kasaliwal, G. R.; Villmow, T. *Polymer* **2012**, *53*, 4.
12. Bauhofer, W. J.; Kovacs, Z. *Compos. Sci. Technol.* **2009**, *69*, 1486.
13. Li, J.; Ma, P. C.; Chow, W. S.; To, C. K.; Tang, B. Z.; Kim, J. K. *Adv. Funct. Mater.* **2007**, *17*, 3207.
14. Ma, P.-C.; Siddiqui, N. A.; Marom, G.; Kim, J.-K. *Compos. Part A: Appl. Sci. Manufact.* **2010**, *41*, 1345.
15. Gunes, I. S.; Jimenez, G. A.; Jana, S. C. *Carbon* **2009**, *47*, 981.
16. Pötschke, P.; Abdel-Goad, M.; Alig, I.; Dudkin, S.; Lellinger, D. *Polymer* **2004**, *45*, 8863.
17. Li, C.; Thostenson, E. T.; Chou, T.-W. *Appl. Phys. Lett.* **2007**, *91*, 223114.
18. Xia, H.; Song, M. *Soft Matter* **2005**, *1*, 386.
19. Sabba, Y. E.; Thomas, L. *Macromolecules* **2004**, *37*, 4815.
20. Xia, H.; Song, M. *J. Mater. Chem.* **2006**, *16*, 1843.
21. Kara, S.; Arda, E.; Dolastir, F.; Pekcan, O. *J. Colloid Interface Sci.* **2010**, *344*, 395.
22. Fei, G.; Tuinea-Bobe, C.; Li, D.; Li, G.; Whiteside, B.; Coates, P.; Xia, H. *RSC Adv.* **2013**, *3*, 24132.
23. Pötschke, P.; Dudkin, S. M.; Alig, I. *Polymer* **2003**, *44*, 5023.
24. Alig, I.; Lellinger, D.; Dudkin, S. M.; Pötschke, P. *Polymer* **2007**, *48*, 1020.
25. Zhang, R.; Dowden, A.; Deng, H.; Baxendale, M.; Peijs, T. *Compos. Sci. Technol.* **2009**, *69*, 1499.
26. Alig, I.; Lellinger, D.; Engel, M.; Skipa, T.; Pötschke, P. *Polymer* **2008**, *49*, 1902.
27. Pötschke, P.; Bhattacharyya, A. R.; Janke, A. *Polymer* **2003**, *44*, 8061.
28. Alig, I.; Skipa, T.; Engel, M.; Lellinger, D.; Pegel, S.; Pötschke, P. *physica status solidi (b)* **2007**, *244*, 4223.

29. Pan, Y.; Cheng, H. K. F.; Li, L.; Chan, S. H.; Zhao, J.; Juay, Y. K. *J. Polym. Sci., Part B: Polym. Phys.* **2010**, *48*, 2238.
30. Zhang, S.; Lin, L.; Deng, H.; Gao, X.; Bilotti, E.; Peijs, T.; Zhang, Q.; Fu, Q. *Colloid. Polym. Sci.* **2012**, *290*, 1393.
31. Cipriano, B. H.; Kota, A. K.; Gershon, A. L.; Laskowski, C. J.; Kashiwagi, T.; Bruck, H. A.; Raghavan, S. R. *Polymer* **2008**, *49*, 4846.
32. Abbasi, S.; Carreau, P. J.; Derdouri, A. *Polymer* **2010**, *51*, 922.
33. Vermogen, A.; Masenelli-Varlot, K.; Séguéla, R.; Duchet-Rumeau, J.; Boucard, S.; Prele, P. *Macromolecules* **2005**, *38*, 9661.
34. Luo, Z. P.; Koo, J. H. *Polymer* **2008**, *49*, 1841.
35. Basu, S. K.; Tewari, A.; Fasulo, P. D.; Rodgers, W. R. *Appl. Phys. Lett.* **2007**, *91*, 053105.
36. Xie, S.; Harkin-Jones, E.; Shen, Y.; Hornsby, P.; McAfee, M.; McNally, T.; Patel, R.; Benkreira, H.; Coates, P. *Mater. Lett.* **2010**, *64*, 185.
37. Peigney, A.; Laurent, C.; Flahaut, E.; Bacsa, R. R.; Rousset, A. *Carbon* **2001**, *39*, 507.
38. Martone, A.; Formicola, C.; Piscitelli, F.; Lavorgna, M.; Zarrelli, M.; Antonucci, V.; Giordano, M. *Express Polym. Lett* **2012**, *6*, 520.
39. Hernández, J. J.; García-Gutiérrez, M. C.; Nogales, A.; Rueda, D. R.; Ezquerra, T. A. *Compos. Sci. Technol.* **2006**, *66*, 2629.
40. Ezquerra Sanz, T. A.; García-Gutiérrez, M. C.; Hernández, J. J.; Nogales Ruiz, A.; Rueda, D. R. *Dispersión de rayos X aplicado al análisis de nanotubos de carbono, polímeros y nanocompuestos*, **2007**.
41. Faiella, G.; Piscitelli, F.; Lavorgna, M.; Antonucci, V.; Giordano, M. *Appl. Phys. Lett.* **2009**, *95*, 153106.
42. Wang, B. N.; Bennett, R. D.; Verploegen, E.; Hart, A. J.; Cohen, R. E. *J. Phys. Chem. C* **2007**, *111*, 5859.
43. Gao, Y.; Li, L.; Tan, P.; Liu, L.; Zhang, Z. *Chin. Sci. Bull.* **2010**, *55*, 3978.
44. Hadjiev, V. G.; Warren, G. L.; Sun, L.; Davis, D. C.; Lagoudas, D. C.; Sue, H. J. *Carbon* **2010**, *48*, 1750.
45. Lucas, M.; Young, R. J. *Compos. Sci. Technol.* **2007**, *67*, 840.
46. Tishkova, V.; Raynal, P.-I.; Puech, P.; Lonjon, A.; Fournier, M. L.; Demont, P.; Flahaut, E.; Bacsa, W. *Compos. Sci. Technol.* **2011**, *71*, 1326.
47. Simmons, J. G. *J. Appl. Phys.* **1963**, *34*, 1793.
48. Yu, Y.; Song, G.; Sun, L. *J. Appl. Phys.* **2010**, *108*, 084319.
49. Allaoui, A.; Hoa, S. V.; Pugh, M. D. *Compos. Sci. Technol.* **2008**, *68*, 410.
50. Takeda, T.; Shindo, Y.; Kuronuma, Y.; Narita, F. *Polymer* **2011**, *52*, 3852.
51. Deng, F.; Zheng, Q.-S. *Appl. Phys. Lett.* **2008**, *92*, 071902.